INTL JOURNAL OF ELECTRONICS AND TELECOMMUNICATIONS, 2011, VOL. 57, NO. 3, PP. 389–393
Manuscript received July 6, 2011; revised August 2011. DOI: 10.2478/v10177-011-0053-4

Experimental Investigation of Factors Affecting Stability of Interferometric Measurements with Ground Based Noise Waveform SAR

Konstantin A. Lukin, Volodymyr P. Palamarchuk, Pavlo L. Vyplavin, and Volodymyr V. Kudriashov

***Abstract*—Application of ground-based SAR and differential interferometry technique is often used for monitoring manmade objects aiming detection of their structural changes. Recently Ka-band Ground Based Noise Waveform SAR has been developed [1] which may be applied for the above monitoring. The paper is devoted to investigation of stability of Noise Waveform SAR. Monitoring of a simple construction has been carried out. The related measurements enabled estimating the accuracy of differential phase measurements using the above Ka-band Noise Waveform SAR. In the paper we present some results of the experiments and their explanations.**

***Keywords*—Noise waveform, noise radar, SAR imaging, differential interferometry.**

I. Introduction

RADAR imaging and interferometry are applicable in many tasks of remote sensing and monitoring of various constructions. One of the promising applications is ground based SAR and differential interferometry. SAR systems preserve phase information about the scattered signals. The obtained images are coherent which means that each image element contains phase information along the amplitude one. This phase information is used in inteferometry to visualize difference between coherent images obtained under different conditions. Differential interferometry is based upon comparison of two coherent images of the same scene made from the same aperture but at different time. If the scene and the equipment don't change between two measurements, the phase difference between coherent images is expected to be equal to zero. If certain changes occur in the scene during the time between taking images, they can be detected in the interferogram as phase shift assigned to the corresponding image pixels. But if the equipment performance or even position has changed with time, some phase shifts can occur in the radio holograms obtained. Such phase shift can impede detection of changes in the object. Sources of instabilities in equipment can be split into two groups: mechanical and electronic ones. Mechanical instabilities have been investigated theoretically in previous works [2]. Current work is devoted to experimental investigation of electronic instabilities in specific SAR – namely, Ka-band Ground Based Noise Waveform SAR (GB NW SAR) [1]. This SAR uses noise signals for sounding and coherent reception of radar returns [3]. We describe the equipment, experimental setup and present the results of NW SAR stability investigation.

The authors are with the Laboratory for Nonlinear Dynamics of Electronic Systems (LNDES), Usikov Institute for Radiophysics and Electronics, NAS of Ukraine, IRE NASU 12 Acad. Proskura St., 61085 Kharkov, Ukraine (e-mails: lukin.konstantin@gmail.com, palmarchuk@mail.ru, pavlo.vyplavin@gmail.com, kudriashovvladimir@gmail.com).

II. Noise Waveform SAR

Coherent images were formed using a Ka-band GB NW SAR operating in bistatic configuration. Tape scanner antennas with synthetic aperture were used for scanning [4]. For the antenna beam forming and scanning in these antennas we use the principle similar to that used in 1D Antenna Array (1D-AA), but realizing transmit/receive of electromagnetic signals at each position of a single radiating element moving along the aperture rather than simultaneous transmit/receive by all its elements. In other words, we use the concept of synthetic aperture radar being applied in the situation of a 1D-AA having a real aperture and implementing sequential radiation of radar signals by its elements. Generally, this approach enables application of both various types of radiating element and methods for implementing of its motion along the antenna aperture. In the antenna suggested, the overall beam width is defined by the antenna real aperture, while the number of beam positions is defined by that of measurement positions for the radiating slot. The sidelobes level depends on the phase-amplitude distribution (weighting function) along the real aperture of the antenna. Technically this approach was realized as follows: As a real aperture antenna, we used a waveguide with a non-radiating half-wavelength longitudinal slot in its wider wall. When covering this wall with a metallic tape having a half-wavelength transverse resonant slot one provides a good condition for resonant radiation of the wave traveling inside the above waveguide. In order to enhance its efficiency we placed a sliding plunger tied to the tape at the proper distance from the radiating slot. The tapes were moved forward and back in step-like manner which simplifies realization of the required synchronous motion of radiating slots in Tx and Rx antennas for the case of bistatic radar configuration. Transmission and reception are done when both antennas are not moving. The tape moves along precise guides. Position of the slot is controlled by angle sensor. Length of synthetic aperture for both antennas equals to 0.7 m.

Frequency modulation technique was applied for sounding noise signal forming: amplified avalanche discharge noise was used as a modulating signal for Ka-band VCO in the noise radar transmitter. The generated signal may have either Gaussian or close to rectangular power spectral density

TABLE I
PERFORMANCE OF KA-BAND GROUND BASED NOISE WAVEFORM SAR

Ka-band GB NW SAR performance	
Working frequencies, GHz	36,5-37
ADC Sampling rate, Gs /sec	1.0
Power Spectrum Bandwidth at -3 dB level, GHz	0.5
Waveform	Noise
Antenna pattern width in elevation & azimuth, deg	20 & 80
Synthetic aperture length, m	0.7
Cross-range resolutionat 50 m distance, m	0.3
Range resolution, m	0.3

shape depending on the modulating signal parameters. High frequency signal from the VCO is amplified and transmitted to the scene in CW regime. Part of that signal is coupled from the transmitter for further usage as a reference. Both radar return and reference signals are amplified and down converted to IF band and digitized with the 8 bit fast ADC with bandwidth 500 MHz (GaGe CompuScope CS82G-1GHz -8M).

Common LO is used for down-conversion of both the reference and the radar returns. Long term frequency stability of the LO is 10^{-9}. RF isolation of the transmit and receive channels is provided by the LO scheme where the oscillations frequency of common X-band oscillator is multiplied by factor of 4 separately in the reference and the receive channels for their down conversions [3] Main performance of the Ka-band GB NW SAR are given in Table I.

III. SAR IMAGING

SAR image formation has been done using straight forward range-Doppler algorithm. As transmit and receive antennas were not moving during transmission and reception of the signals, imaging could be split into range and azimuth compression steps.

Let's consider range compression. Assume that a point-like target exists the in the observed space at coordinates (x, y), range from the transmitter to this target is $l_{Tx.}(x, y)$, while range from the receiver to this target is $l_{Rx.}(x, y)$. Total duration of radar signal propagation from the transmitter to the target and from target to transmitter $\tau(x, y)$ equals:

$$\tau(x, y) = \frac{l_{Tx.}(x, y) + l_{Rx.}(x, y)}{c}, \quad (1)$$

where c is radio wave propagation velocity (we assume space to be uniform and neglect dispersion properties of the medium and consider constant propagation velocity). Antennas in the system move synchronously preserving the same distance between them. Radiation and transmission are done at quantized positions of antennas. Propagation time of form (1) can be assigned to each position a of the antennas:

$$\tau_a(x, y) = \frac{l_{Tx.a}(x, y) + l_{Rx.a}(x, y)}{c}. \quad (2)$$

This time describes delay of the reflected by the considered target signal with respect to the stored as reference transmitted signal taken at the output of the transmitter.

Correlation processing is normally used for noise signals. Evaluation of correlation is $\hat{R}_a(T)$ between radar return $S^*_{Rx.a}(t + \tau_a(x, y))$ and reference signal is to be done as:

$$\hat{R}_a(\tau) = \lim_{T\to\infty} \frac{1}{T} \cdot \int_0^T S_{Tx.a}(t + \tau) \cdot S^*_{Rx.a}(t + \tau_a) d\tau, \quad (3)$$

where time of averaging is T, τ is delay of the sounding signal, *denotes complex conjugation. Infinite integration period cannot be realized in practice. Thus, correlation can be only estimated. Precision of the estimation depends on the signal time-bandwidth product [3]. Set of $\hat{R}_a(\tau)$ for all antenna positions a and all necessary mutual delays τ is called range compressed data [5].

Because in the described system signal has to propagate in the waveguides of scanning antennas and length of these waveguides changes during scanning, range compression has to take into account this propagation. Such correction can be done in spectral domain using known relation for propagation constant of rectangular waveguide [6]:

$$C_{10}(w_i) = 2\pi \cdot \sqrt{\frac{\epsilon \cdot \mu}{\lambda^2} - \frac{1}{2 \cdot p^2}}, \quad (4)$$

where p is size of wide wall of the waveguide. Phase shift of each spectral component of the signal due to propagation in waveguide is equal:

$$\varphi_a(w_i) = e^{j \cdot l_a \cdot 2C_{10}(w_i)}, \quad (5)$$

where l_a is total length of the waveguides at antenna position a. Using this correction along with estimation of cross correlation in spectral domain can be done as:

$$\hat{R}_a(\tau) = \sum_{w_{min}}^{w_{max}} |S_{Tx.a}(w_i)|^* \cdot \left| \frac{S_{Rx.a}(w_i)}{\varphi_a(w_i)} \right| \cdot e^{j \cdot w_i \cdot \tau} \quad (6)$$

Relation (6) can be derived using Parseval's theorem. Besides phase correction, estimation of cross-correlation in spectral domain provides higher computational effectiveness than that in time domain (3). Maximum of the estimation (for the case of single point-like target) corresponds to the delay $S_{Tx.a}(t + \tau)$, at which mutual delay of the signals is compensated: $\tau = \tau_a$. Width of the estimation peak equals $\frac{c}{2\Delta f}$, where Δf is frequency bandwidth of the sounding signal.

Finiteness of the integration time in cross-correlation estimation leads to random structure of the results which is

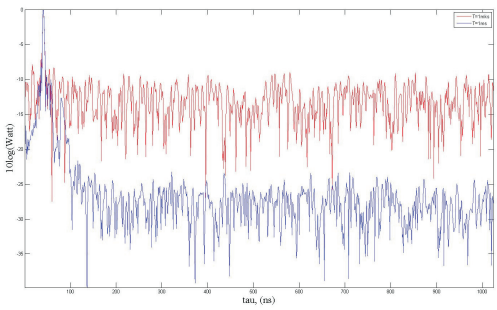

Fig. 1. Estimation of cross-correlation of noise signal (range compressed data for single antenna position). Red line – 1 μs integration. Blue line – 1 ms integration. Bandwidth of the signal is same for both plots $\Delta f_{-3dB} \sim 0.5$GHz.

observed as presence of residual fluctuations in range profiles. Figure 1 illustrates the presence of residual fluctuations and possibility to decrease them via increasing the integration time. It can be seen that at short integration time a weak target may be masked by residual fluctuations from a stronger one and increasing the integration time enables to clearly detect the weak target.

Azimuth compression of the signal is focusing of the synthetic aperture to each element of the image. It is done by summing up signals from all positions of radiating slot taking into account phase shift of the signal due to propagation to the imaged point from [5]:

$$I(x,y) = \sum_{a=1}^{A} \{R[\tau_a(x,y)]\} \cdot e^{j\cdot\omega_0[-\tau_a(x,y)]} \qquad (7)$$

where ω_0 denotes the central circular frequency of the signal.

Figure 2 illustrates dependence of residual fluctuations in SAR image on integration time. The objects visible in the image are described below.

IV. Experimental Setup

The aim of the experiment was to observe phase shifts due to changes in electronic part of the radar. The equipment was placed in the laboratory room. The antenna was aimed upwards and faced edge between ceiling and wall. Two corners were in the field of view of the radar. Crack in ceiling, two metal heating tubes were also in the scene. Transmitter and receiver equipment was mounted on supports standing on the laboratory floor. The system was used in bistatic mode – the scanning antennas were placed at distance 1.5 m from each other (Fig. 3). It was planned to measure phase shifts in SAR interferograms of stable scene as the equipment heats up. Besides, we investigated possibility to use the equipment just after it's turning on following sequence: "turn on, scan, turn off – long wait – turn on, scan, turn off".

The radar was assembled in a way that it could be turned on and left in a closed room. The control of scanning was done remotely. Air conditioner and other equipment potentially influencing radar have been turned off. People didn't enter the room during the experiment. Each day, during first one and a half hour measurements were made each 10-20 minutes. After that measurements were made with interval one hour.

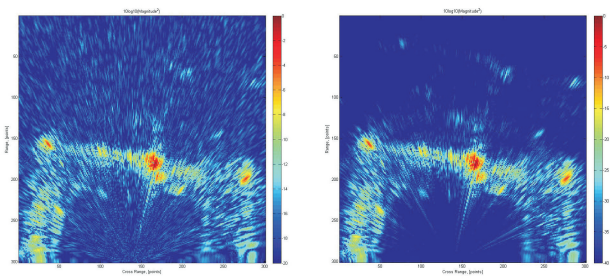

Fig. 2. Radar images for various integration time obtained experimentally. Left image – integration time 1 μs, right image – integration time 1 ms. Bandwidth $\Delta f_{-3dB} \sim 0.5$GHz.

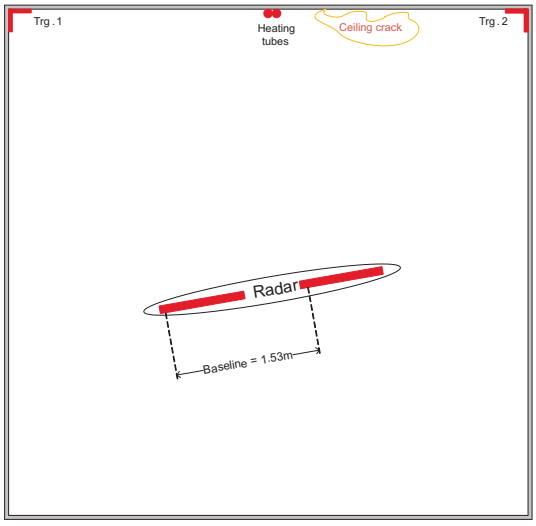

Fig. 3. Diagram for placing of Ka-band Ground Based NW SAR and scene.

During last 30 min of the first day four measurements were made.

Figure 4 shows example of SAR image of the scene of interest. Such objects as edges of the ceiling, metal tubes and corners can be easily seen in the image.

V. Differential Interferometry

Formation of differential interferograms consists in comparison of phases of corresponding pixels of the coherent SAR images obtained at different time. This can be done by multiplication of one image by complex conjugate to another one. Each pixel of the resulting image will have amplitudes equal to product of amplitudes of the initial images and phase factor with differential phase [7]. Figure 5 shows example of differential interferogram obtained using coherent images

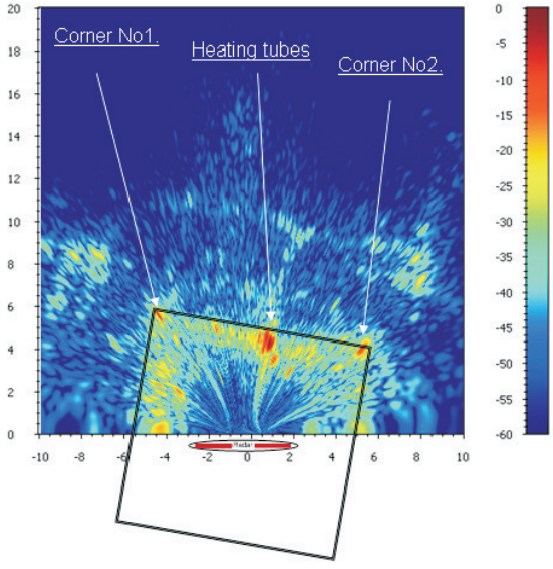

Fig. 4. SAR image of the room ceiling and scheme of radar and scene positioning.

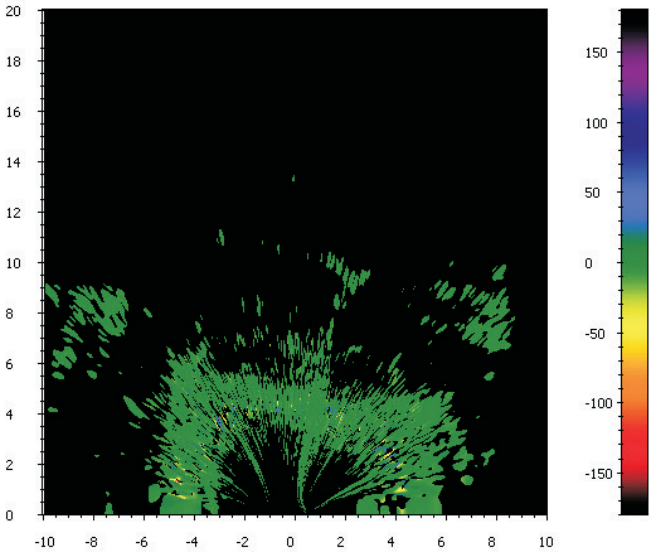

Fig. 5. Differential inteferogram obtained with time base 62 minutes with heated up equipment. Phase shifts are close to zero.

taken in one day with time base 62 minutes with heated up equipment. Phase shifts in this interferograms are close to zero which means absence of strong changes in the equipment and scene. Mean phase on the interferogram is equal to 0, standard deviation is 3 degrees. This means that usage of the elaborated equipment in such mode has an instrumental accuracy of displacements measurements $\sim$ 0.03 mm.

Figure 6a shows example of inteferogram obtained when equipment heating up was in progress: during the first hour of operation with time base equal to 10 minutes. It can be seen that phase changes during this period are quite high. Figure 6b shows corresponding histogram at which both shift of mean phase value and widening of the peak due to phase noise are also seen.

Figure 7 shows time variation of mean phase in inteferogram with heating up. Two lines correspond to two days of measurements (two realizations of heating up). It can be seen that equipment is not stable during first 200 minutes of operation. The fastest variation of phase occurs just after switching on. Two realizations of heating up are similar and finally they end up at the same mean phase value. This means that the equipment can be used in regime "turn on – heat up – scan

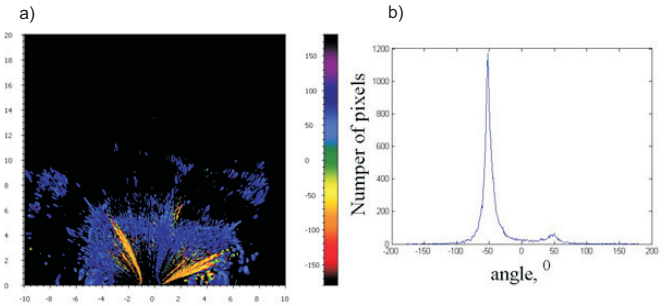

Fig. 6. a) Differential inteferogram obtained during heating up of the equipment; b) Corresponding phase histogram.

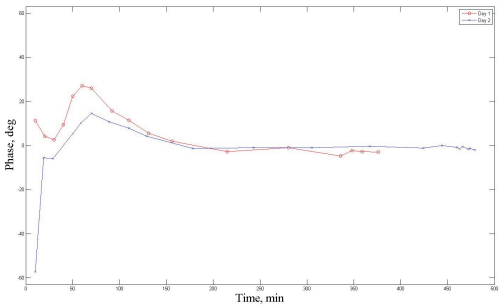

Fig. 7. Dependence of mean phase on time of heating up.

– turn off – long time base – turn on – heat up – scan – turn off". Figure 8 shows example of inteferogram obtained in such regime (time base is equal to one day). Mean phase $\sim 3^0$, standard deviation of phase $\sim 10^0$. This means that usage of the elaborated equipment in this regime limits potential precision of displacement measurement at $\sim$ 0.1 mm.

Observation of reference channel spectra and signals has shown that spectrum shape doesn't change drastically during heating up. Thus, the instabilities are assigned to processes in amplifiers of the radar return channel. Further improvement of the equipment can consist of thermal stabilization of receiver parts which should give shorter heating up times.

VI. Conclusions

In the paper, we presented some results of investigation of precision of phase measurements with Ka-band ground based noise SAR for the differential interferometry applications. The experiments confirmed potential precision of phase shift measurement of 3 degrees. They also showed the limits of such precision and regimes when the phase measurements are not possible. It has been shown that the equipment can be used for

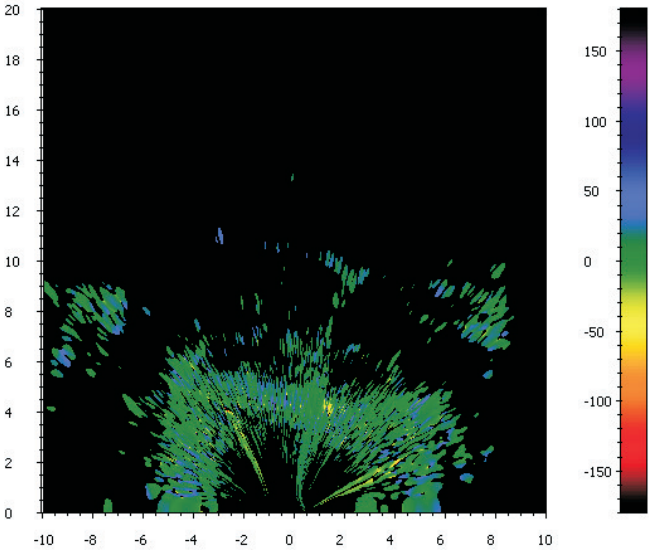

Fig. 8. Differential interferogram obtained on coherent images taken at different days.

long time bases but for that purpose it has to be heated up each time the measurements are carried out. Further improvement of the equipment can consist of thermal stabilization of the NW SAR receiver.

REFERENCES

[1] K. A. Lukin, A. A. Mogyla, V. P. Palamarchuk, P. L. Vyplavin, O. V. Zemlyaniy, Y. A. Shiyan, and N. K. Zaets, "Ka-Band Bistatic Ground-Based Noise Waveform SAR for Short-Range Applications," *IET Radar, Sonar & Navigation*, vol. 2, no. 4, pp. 233–243, 2008.

[2] K. A. Lukin, A. A. Mogyla, and P. L. Vyplavin, "Estimation of phase errors caused by instability of a ground-based sar trajectory," *Applied Radioelectronics. State and development prospects.*, vol. 2, 2005.

[3] K. A. Lukin, "Noise Radar Technology," *Journal of Telecommunications and Radio Engineering*, vol. 55, no. 12, pp. 8–16, 2001.

[4] ——, "Sliding Antennas for Noise Waveform SAR," *Applied Radio Electronics*, vol. 4, no. 1, pp. 103–106, 2005.

[5] J. Curlander and R. McDonough, *Synthetic Aperture Radar: Systems and Signal Processing*. John Wiley & Sons, 1991.

[6] V. V. Nikolskiy and T. I. Nikolskaya, *Electrodynamics and Propagation*. Moscow: Science, 1989.

[7] K. A. Lukin and A. A. Mogyla, "Noise Waveform SAR and Differential Interferometry for Detection of Structural Changes in Chernobyl Sarcophagus," CD only.